



OPEN ACCESS

EDITED BY
Gideon Gal,
Israel Oceanographic and Limnological
Research, Israel

REVIEWED BY
Xiaoshang Ru,
Chinese Academy of Sciences (CAS),
China
Marco Scotti,
National Research Council (CNR), Italy
Rinkesh Wanjari,
Maharashtra Animal and Fishery Sciences
University, India

*CORRESPONDENCE
Xue Feng
✉ fengxue@scsfri.ac.cn
Jiangtao Fan
✉ fjt@scsfri.ac.cn

RECEIVED 12 November 2025
REVISED 04 March 2026
ACCEPTED 06 March 2026
PUBLISHED 25 March 2026

CITATION
Feng X, Hong X, Chen P and Fan J
(2026) Ecosystem characteristics
and ecological carrying capacity
of a subtropical marine ranch
in the pearl river estuary: an
ecopath modeling approach.
Front. Mar. Sci. 13:1744551.
doi: 10.3389/fmars.2026.1744551

COPYRIGHT
© 2026 Feng, Hong, Chen and Fan. This
is an open-access article distributed under
the terms of the [Creative Commons
Attribution License \(CC BY\)](https://creativecommons.org/licenses/by/4.0/). The use,
distribution or reproduction in other
forums is permitted, provided the
original author(s) and the copyright
owner(s) are credited and that the
original publication in this journal is
cited, in accordance with accepted
academic practice. No use, distribution
or reproduction is permitted which does
not comply with these terms.

Ecosystem characteristics and ecological carrying capacity of a subtropical marine ranch in the pearl river estuary: an ecopath modeling approach

Xue Feng^{1,2,3*}, Xiaofan Hong⁴, Pimao Chen^{1,2,3} and Jiangtao Fan^{1,5*}

¹South China Sea Fisheries Research Institute, Chinese Academy of Fishery Sciences, Guangzhou, China, ²Key Laboratory of Marine Ranching, Ministry of Agriculture and Rural Affairs, Guangzhou, China, ³Scientific Observing and Experimental Station of South China Sea Fishery Resources and Environments, Ministry of Agriculture and Rural Affairs, Guangzhou, China, ⁴Zhangzhou Talent Development Group, Zhangzhou, China, ⁵Key Laboratory for Sustainable Utilization of Open-Sea Fishery, Ministry of Agriculture and Rural Affairs, Guangzhou, China

Marine ranching has been widely promoted as an ecosystem-based approach to restore degraded coastal ecosystems and enhance fishery resources, particularly in heavily impacted estuarine regions. The National Marine Ranch Demonstration Zone of Wailingding Island, located in the Pearl River Estuary of the northern South China Sea, represents a typical subtropical coastal system influenced by intensive anthropogenic activities and ecological restoration efforts. Based on continuous bottom trawl surveys in April and September 2020 from the Wailingding Island marine ranch (WIMR) area, this study employed an Ecopath model to evaluate the ecosystem characteristics of the study area. The model systematically analyzed energy flows, structural characteristics, and the ecological carrying capacity of major functional groups. Seventeen functional groups were defined, representing the key energy transfer pathways in the study area. Their trophic levels (TLs) ranged from 1.000 to 3.737, with marine mammals occupying the highest level. The overall energy transfer efficiency of the ecosystem was 3.873%, and the total system throughput reached 10,536.750 t/(km²·year), with 49% derived from detritus. The ratios of total primary production to total respiration (TPP/TR) was 7.431. Finn's cycling index (FCI) and Finn's mean path length (FML) were 2.529% and 2.198. These results suggest that the Wailingding Island marine ranch ecosystem is characterized by low maturity and stability and a relatively simple food web structure. Model simulations further indicated that under ecologically balanced conditions, the ecological carrying capacities of major functional groups could increase up to 3.8 times their current biomass levels.

KEYWORDS

ecological carrying capacity, ecopath model, ecosystem structure, marine ranch, pearl river estuary

1 Introduction

To mitigate ecosystem degradation and the decline of fishery resources, the construction of modern marine ranches has become a key strategy for promoting the transformation and upgrading of coastal fisheries (Zhou et al., 2021). Marine ranching projects, including artificial reef deployment, scientifically guided stock enhancement and release, the strengthening of resource management, and habitat enhancement (Liu, 2022), have expanded rapidly in recent decades, especially in China (Chen et al., 2020). As a vital component of China's marine ecological civilization, marine ranches play an important role in conserving and restoring marine environments and enhancing fishery resources. They not only provide an effective means to protect aquatic biological resources and rehabilitate degraded habitats, but also serve as an essential pathway toward the sustainable development of coastal fisheries (Yuan and He, 2022). While some studies report increases in food web complexity and species richness (Song et al., 2022; Nauta et al., 2023; Feng et al., 2025), others suggest that artificial structures may alter trophic pathways, intensify competition, or increase reliance on detrital energy flows (Heery et al., 2018; Reeds et al., 2018; Zhang et al., 2022). Consequently, evaluating the ecosystem-level responses of marine ranch systems has become essential for understanding whether such interventions genuinely promote ecosystem recovery or merely redistribute biomass within existing food webs.

The Pearl River estuary, located in the northern South China Sea, is one of the most economically developed and ecologically stressed coastal regions in China, supporting abundant coastal fishery resources (Peng et al., 2019). As the main convergence zone between the Pearl River runoff and offshore waters of the South China Sea, this region possesses unique hydrological and nutrient conditions, making it an essential fishing ground and natural spawning site for numerous economically important fish species (Zhang et al., 2011). However, due to its proximity to the highly developed Pearl River delta, the estuary has also become a major maritime transportation corridor. Pollutants discharged from ships and land-based sources have caused severe marine pollution, while nutrient enrichment from anthropogenic inputs has led to eutrophication, making this one of the most red tide-prone areas in China (Si, 2018). In recent years, several biological resource surveys have been conducted in the Pearl River Estuary to evaluate ecosystem conditions and assess the effectiveness of marine ranch construction (Zhang et al., 2011; Yuan et al., 2017; Peng et al., 2019). Although some studies have analyzed the community structure of marine organisms, the overall ecosystem characteristics and ecological carrying capacities of key functional groups in the estuarine marine ranch areas remain poorly understood. The Wailingding Island National Marine Ranch Demonstration Zone, located in the estuarine-coastal transition zone of the Pearl River estuary, represents a typical subtropical marine ranch system influenced by both ecological restoration measures and strong anthropogenic disturbances (Xie et al., 2022). Understanding the trophic structure and functioning of this system is therefore critical for evaluating the effectiveness of marine ranching practices in estuarine contexts.

Ecopath with Ecosim (EwE) suite of models is widely used for quantitative assessments of marine food webs and ecosystem-based management (Craig and Link, 2023; Keramidas et al., 2023). The operating principle of the Ecopath component in EwE is based on thermodynamics, the ecosystem is simplified by constructing a food web in the model, with various ecosystem characteristics quantified through modeling (Heymans et al., 2016). Recent advances in ecosystem modeling using EwE have expanded its application to evaluate ecological outcomes of restoration and management in coastal and estuarine systems (de Mutsert et al., 2021; Wang et al., 2024b). Multiple regional and global studies have emphasized improved calibration practices, uncertainty quantification, and the use of network indicators to interpret ecosystem maturity and resilience (Heymans et al., 2016; Susini and Todd, 2021; Bentley et al., 2024; Saygu et al., 2025). In particular, EwE-based assessments applied to marine ranching and stock-enhancement projects have highlighted both potential benefits for biomass recovery and limitations associated with trophic constraints and detritus-dominated pathways (Wang et al., 2022b; Zhang et al., 2022; Yan et al., 2025). These recent findings motivate our ecosystem modeling of the Wailingding Island marine ranch area and underscore the need to combine field surveys with model-based diagnostics when informing ecosystem-based management decisions in heavily impacted estuarine environments.

Therefore, in this study, based on fishery resource survey data from the National marine ranch demonstration zone of Wailingding Island, Zhuhai, Guangdong Province, we developed an Ecopath model of the local ecosystem using EwE software. The objectives were to (1) analyze the food web structure and energy flow patterns, (2) quantitatively evaluate the overall ecological characteristics of the system, and (3) estimate the ecological carrying capacities (ECC) of key functional groups in the demonstration area. The results aim to provide baseline ecological data for assessing the ecological effectiveness of marine ranch construction and to support the management and conservation of coastal fishery resources in China.

2 Materials and methods

2.1 Study area and sample collection

The National Marine Ranch Demonstration Zone of Wailingding Island is established in the eastern side of the Wanshan Archipelago, Zhuhai City, Guangdong Province, China. The surveyed area extends from 114°02' to 114°06' E and 22°05' to 22°07' N. To improve the ecological environment and conserve local fishery resources, a total of 1,781 artificial reef units have been deployed in recent years, with a combined reef volume of 37,497 m³. These structures include multifunctional bait reefs made of reinforced concrete, trapezoidal algal reefs, and associated facilities such as seaweed cultivation zones covering approximately 6.25 hectares. The entire demonstration area covers about 2.16 km² (Feng et al., 2021).

Biological surveys were conducted at 12 sampling stations within the study area in April and September 2020 (Figure 1). Considering that the study area is located in an open coastal estuarine region and the aggregation effects of artificial reefs on marine organisms, the sampling scheme of the study consisted of nine stations (S1-S9) within the artificial reef area and three stations (S10-S12) in adjacent waters, in order to minimize model simulation errors caused by animal migration. Sampling was carried out using a trawl fishing vessel (*Yuedongguan Fishing 92008*) equipped with a bottom trawl net (head rope: 36 m, foot rope: 31 m, mesh size: 3–5 cm). The towing speed ranged from 2.7 to 2.8 knots, and each trawl lasted for 15 minutes. Given that the sampling stations in the study area were located relatively close to each other, in the actual sampling process, we primarily adopted repeated trawling centered around the stations, and even conducted non-continuous trawling to avoid nearshore reefs. Sampling stations were used as reference starting points rather than fixed sampling points. Sampling, processing, and analysis were conducted in accordance with the *National Standards of the People's Republic of China — Specification for Oceanographic Survey, Part 6: Marine Biological Survey* (GB/T 12763.6–2007). A total of 48 species were recorded across the two field surveys, comprising 1 species of cartilaginous fish, 36 species of bony fish, 9 species of crustaceans, and 2 species of cephalopods, and all biological samples collected were processed through laboratory experiments to determine key biological information, including taxonomy, body size, and stomach contents.

2.2 Construction of the ecopath model

2.2.1 Modeling principles of the ecopath model

We constructed an Ecopath model to represent the average annual conditions in 2020 for the WIMR ecosystem with EwE (v.6.7.0) software (Christensen et al., 2005). In the Ecopath model, functional groups with similar trophic levels (TLs), life histories, and niche characteristics (including diet, size, habitat preference, etc.) must be comprehensively considered (Pauly et al., 2000), and all functional groups must include basic processes of energy and material flow in the ecosystem (Christensen and Pauly, 1992). Ecopath comprises two main equations (Eq.)—the first, Eq. (1),

defines the balance between the input and output of each functional group to ensure that the ecotrophic efficiency (EE) does not exceed 1; Eq. (2) defines the thermodynamics of the functional groups. The expressions of Equations 1, 2 are:

$$B_i \cdot (P/B)_i \cdot EE_i = Y_i + \sum_{j=1}^n B_j \cdot (Q/B)_j \cdot DC_{ij} + B_i \cdot BA_i + E_i \quad (1)$$

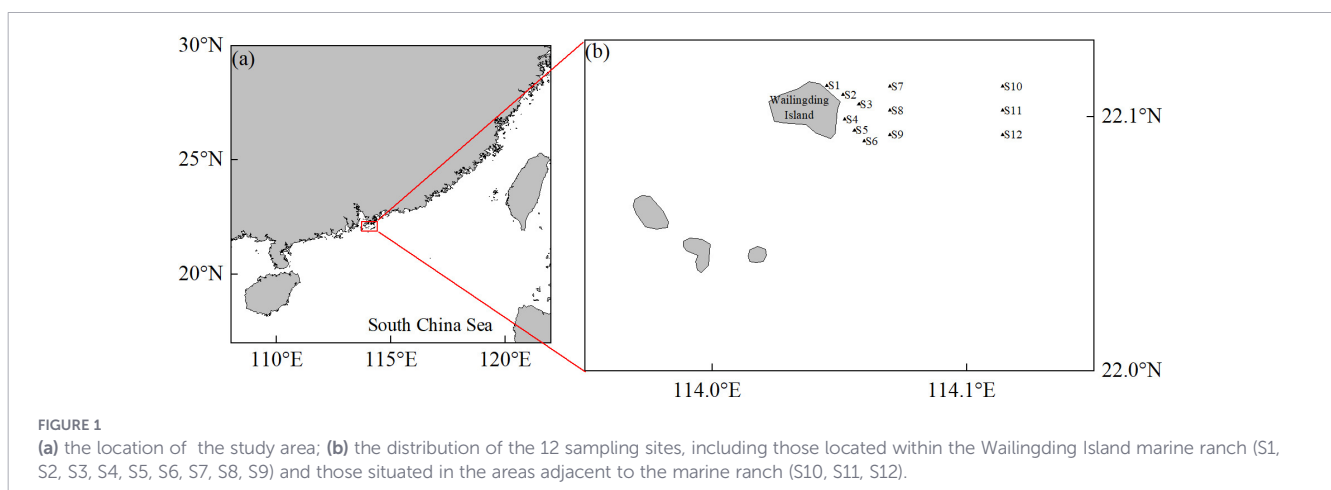
$$Q_i = P_i + R_i + U_i \quad (2)$$

where B_i is the biomass of group i ; $(P/B)_i$ is the production of group i per unit biomass, equal to the total mortality rate of group i ; EE_i is the ecotrophic efficiency of group i , defined as the fraction of production that is consumed within the system or removed by fishers; Y_i is the total fishery catch rate of group i ; $(Q/B)_j$ is the consumption rate of group j per unit biomass; DC_{ij} is the fraction of prey i in the average diet of predator j ; BA_i is the biomass accumulation rate of group i ; E_i is the net migration rate (immigration and emigration); Q_i is the consumption of group i ; R_i is the respiration of group i ; and U_i is the unassimilated food of group i (Christensen et al., 2008).

2.2.2 Functional group classification

Within the Ecopath framework, an ecosystem is conceptualized as a network of biologically related functional groups that interact through trophic relationships. The number of groups typically ranges between 13 and 50, representing the major processes of energy and material flow in the ecosystem (Christensen and Pauly, 1992). Recognition of Ecopath functional groups requires consideration of shifts in the habitat of life history stages and/or diet. Finally, functional groups are represented as single biomass pools or multi-stanza functional groups (Walters et al., 2008).

The classification of functional groups in this study is primarily based on biological data obtained from field sampling. Except for the results of field investigation, these functional groups are also selected based on characteristics of ecology, biosystematics, diets of species, and species distributions in the WIMR area (Chen and Qiu, 2010; Sun et al., 2016; Liu et al., 2019b). Finally, we also referenced existing Ecopath models developed for adjacent marine ecosystems with similar environmental conditions. The Ecopath model of



WIMR ecosystem was divided into 17 functional groups. The species of fish are assigned to functional groups according to similar ecological characteristics (e.g., diet, predators, body sizes, and metabolic requirements), for example the group names of demersal fish functional groups are assigned based on size (small, medium and large). These groups comprehensively represent different TLs and energy flow pathways within the marine ranch ecosystem (Table 1).

2.2.3 Model parameterization and data sources

In the Ecopath model developed for this study, energy flow within the system was expressed as material transfer (biomass, wet weight, t/km²) over an annual time frame. The biomass of phytoplankton was estimated from measured chlorophyll *a* concentrations in the study area (Liu et al., 2017), while bacterial biomass was assumed to be 17.5% of the phytoplankton biomass (Liu et al., 2019a). Zooplankton biomass was converted to wet weight based on survey data from the Pearl River Estuary (Hong et al., 2022).

Due to the absence of field data for seaweeds—one of the main benthic primary producers—their biomass was estimated using a preliminary ecotrophic efficiency (0.5, *EE*) value derived from comparable ecosystems (Liu et al., 2019b). Detritus biomass was estimated using an empirical Equation 3 based on primary productivity and euphotic zone depth in the study area (Pauly et al., 1993).

$$\log D = -2.41 + 0.954 \log PP + 0.863 \log E \quad (3)$$

where *D* represented the total amount of organic detritus (gC/m²); *PP* represented primary productivity (gC/m²/year); *E* represented the euphotic zone depth.

The biomasses of seabirds, marine mammals, and jellyfish were obtained from survey data in the same or adjacent marine regions (Chen and Qiu, 2010; Sun et al., 2016; Huang et al., 2019), and biomass data for the remaining functional groups (fish and crustaceans) were directly derived from the average stock density obtained from field surveys conducted in the Wailingding Island Marine Ranch (WIMR) area in 2020. These densities were calculated as the ratio of the total weight of biological samples to the total trawled area.

The production-to-biomass (*P/B*, year⁻¹) and consumption-to-biomass (*Q/B*, year⁻¹) ratios for fish groups were estimated using empirical Equation 4 and validated against the FishBase database (<https://www.fishbase.se>).

$$\log(Q/B) = 7.964 - 0.204 \log W - \frac{1965}{T} + 0.083A \quad (4)$$

where *W* mean the asymptotic weight of fish species (g), *T* was the mean value of water temperature (K) in the study area, *A* was the aspect ratio of fish species (Palomares and Pauly, 1998).

For functional groups with parameters lacking local measurements (e.g., *P/B* and *Q/B* values), we selected reference values from validated Ecopath models developed for subtropical coastal and similar artificial reef ecosystems with similar species composition and trophic structure, including other areas within the Pearl River Estuary (Liu et al., 2019b) and the Beibu Gulf (Chen and Qiu, 2010; Sun et al., 2016; Feng et al., 2025), also located in the

TABLE 1 Functional groups and representative species in Wailingding Island marine ranch.

Number	Functional group	Main species
1	Seabirds	Charadriidae, Apodidae, Jacanidae, Laridae, etc.
2	Marine mammals	Delphinidae, <i>Neophocaena</i> , <i>Dugong dugon</i> , etc.
3	Cartilaginous fishes	<i>Scoliodon sorrakowah</i> , etc.
4	Small benthic invertebrates	Bivalvia, Gastropoda, Polychaeta, Echinodermata, etc.
5	Benthic crustaceans	<i>Scylla serrata</i> , <i>Portunus sanguinolentus</i> , <i>Charybdis japonica</i> , <i>Charybdis feriatius</i> , <i>Metapenaeus affinis</i> , <i>Metapenaeus joyneri</i> , <i>Banana prawn</i> , <i>Penaeus penicillatus</i> , <i>Penaeus monodon</i> , <i>Oratosquilla kempii</i> , <i>Harpisquilla harpax</i> , <i>Oratosquilla oratoria</i> , etc.
6	Cephalopods	<i>Loligo edulis</i> , <i>Loligo duvaucelii</i> , <i>Loligo chinensis</i> , etc.
7	Large pelagic fishes	<i>Trichiurus lepturus</i> , Sphyrnidae, etc.
8	Small pelagic fishes	<i>Decapterus maruadsi</i> , <i>Ilisha melastoma</i> , <i>Lactarius lactarius</i> , <i>Thryssa kammalensis</i> , etc.
9	Large demersal fishes	Pleuronectiformes, Aluteridae, <i>Lagocephalu</i> , etc.
10	Medium demersal fishes	<i>Siganus oramin</i> , <i>Mugil cephalus</i> , <i>Psenopsis anomala</i> , <i>Clupanodon punctatus</i> , etc.
11	Small demersal fishes	Leiognathidae, Apogonidae, Acropomatidae, Gobiidae, Scorpaenidae, etc.
12	Jellyfish	Coelenterata, Ctenophora, etc.
13	Zooplankton	Copepods, Chaetognatha, Cladocera, etc.
14	Bacteria	Heterotroph bacteria
15	Seaweeds	Marine alga, seagrass
16	Phytoplankton	Bacillariophyta, Pyrrophyta, Cyanophyta, Chlorophyta, etc.
17	Detritus	Particulate organic carbon, Dissolved organic carbon, etc.

northern South China Sea. In addition, we compared and adjusted parameters based on studies from other artificial reef zones along the Chinese coast (Liu et al., 2019a; Zhang et al., 2022; Wang et al., 2024b; Yan et al., 2025), following best-practice recommendations for model calibration and documentation (Coll  ter et al., 2013). Sensitivity of results to selected parameter values was evaluated via the EwE pedigree and pre-balance diagnostics.

Diet composition matrices were compiled using a combination of local stomach-content data based on laboratory observations, FishBase (<https://www.fishbase.org>) trophic summaries, and additional peer-reviewed diet studies from adjacent coastal ecosystems (Chen and Qiu, 2010; Sun et al., 2016; Liu et al., 2019a, Liu et al., 2019b; Feng et al., 2025); where local data were absent, diet proportions were informed by ecologically similar models in EcoBase (Coll  ter et al., 2013) and refined through expert consultation, ensuring realistic trophic linkages and consistency with empirical ecological data. A ‘‘diet import’’ approach was needed for some functional groups given the WIMR area represents an open ecosystem (Christensen et al., 2008). Therefore, biological differences rendered animals with stronger migratory abilities to have greater potential to obtain food from other ecosystems. In this study, the exogenous energy import in the diet matrix for seabirds, marine mammals, cartilaginous fish, and large pelagic fish was set at 0.396, 0.351, 0.235, and 0.157, respectively (Supplementary Table 1).

2.2.4 Model construction and model balancing

A pre-balancing (PREBAL) diagnostic test was applied prior to model balancing to assess internal consistency following Link (2010). The diagnostic process evaluated biomass distribution, production ratios, and system-level energy flows. According to thermodynamics, the Ecopath model after a PREBAL diagnostic is adjusted to reach a state of equilibrium. Output parameters requiring adjustment include: EE (< 1.0), gross good conversion efficiency (P/Q , $0.1-0.3$), net efficiency (NE , $NE-P/Q > 0$), respiration/assimilation biomass (R/AS , < 1.0), respiration/biomass (R/B , fish: $1-10$; high conversion efficiency population: $50-100$), and production/respiration (P/R , < 1.0 or > 1.0) (Link, 2010; Heymans et al., 2016).

To achieve a balanced steady-state model, all input parameters were iteratively adjusted to maintain consistency between energy inputs and outputs in accordance with ecological and thermodynamic principles (Heymans et al., 2016). The model was parameterized using field sampling data, including biomass estimates and species composition, to inform functional group definition and initial biomass inputs. Model performance was evaluated through mass-balance requirements (i.e., $EE \leq 1.0$ for all functional groups), parameter consistency checks, and PREBAL diagnostics following established best practices (Link, 2010). Together, these procedures ensured that energy flows and trophic interactions in the model were internally consistent and ecologically reasonable under steady-state assumptions. The Pedigree index embedded in EwE (v.6.7.0) was used to quantify the reliability of parameter sources and evaluate the overall quality of the model (Christensen and Walters, 2004).

2.3 Trophic structure analysis

Mixed trophic impact (MTI) analysis was used to quantify direct and indirect trophic effects among functional groups, revealing how changes in one group’s biomass influence others (Ulanowicz and Puccia, 1990), it is calculated as follows (Equation 5):

$$MTI_{ji} = DC_{ji} - FC_{ij} \quad (5)$$

where MTI_{ji} is the interaction between the impacting functional group j and the impacted functional group i , DC_{ji} is the fraction of prey j in the diet of predator i , and FC_{ij} is a host composition term giving the proportion of the predation on i because of j as a predator.

Based on mixed trophic impact, keystone species analysis was conducted to identify species or groups that, despite having relatively low biomass, exert disproportionately large effects on ecosystem structure and stability (Power et al., 1996; Libralato et al., 2006), the specific calculation equations are shown in Equations 6–7 below:

$$\varepsilon_i = \sqrt{\sum_{j \neq i}^n MTI_{ij}^2} \quad (6)$$

$$KS_i = \log[\varepsilon_i(1 - p_i)] \quad (7)$$

where ε_i is the total impact of functional group i on the ecosystem by estimating through the MTI, KS_i is the keystone index of functional group i , and p_i is the contribution of functional group i to the total food web biomass.

Additionally, we examined resource competition among functional groups using the niche overlap index (OI) incorporated in the EwE software, with the formula as follows (Equation 8):

$$OI_i = \sum_{j=1}^n (p_{ji} \cdot p_{ki}) / (\sum_{j=1}^n (p_{ji}^2 \cdot p_{ki}^2) / 2) \quad (8)$$

here, P_{ji} and P_{ki} represent the proportions of the resource i used by functional groups j and k , respectively. The index is symmetrical and assumes values between 0 and 1.

2.4 Ecological indicators in the model

The output ecological indicators of the Ecopath model were used to describe the ecosystem’s size, stability, and maturity. Specifically, we quantified the overall characteristics of the ecosystem by evaluating key ecological indicators, such as total system throughput (TST ($t/(km^2 \cdot year)$), the total flow of matter through all compartments of an ecosystem), total primary production (TPP , the total amount of energy or carbon fixed by autotrophs (plants, algae, bacteria) through photosynthesis in an ecosystem, known as gross primary production), and total biomass (TB , standing stock excluding detritus), the TST comprises total consumption (TC , the total amount of energy that all consumers in an ecosystem obtain from lower trophic levels or detritus), total exports (TEX , the total amount of energy or matter that flows from within an ecosystem to an external system), total respiration (TR , the total amount of energy released by all living organisms in an ecosystem through respiration to maintain their life activities), total

flow to detritus (*TFD*, the total amount of energy or biomass produced by all biological components in an ecosystem and entering the “detritus” reservoir). These indicators are essential for assessing the overall activity and size of the ecosystem.

The ratios of *TPP/TB* (an immature system accumulates biomass because production exceeds respiration) and *TPP/TR* (a value below 1 indicates high environmental stress, while a value above 1 suggests that the system remains in an early developmental stage and is immature) were determined to measure the stability and maturity of the ecosystem (Odum, 1969). Additional indices such as the Finn’s cycling index (FCI, quantifies the proportion of an ecosystem’s throughput that undergoes recycling) and Finn’s mean path length (FML, the average number of groups an inflow or outflow passes through) were also used to assess ecosystem complexity and energy recycling efficiency (Odum, 1969).

At the same time, mean transfer efficiency (mTE) within trophic levels (TLs) measures the efficiency of energy utilization at each trophic level in the system (Christensen et al., 2008), the Shannon diversity index estimates species diversity by considering the quantity of species present in a habitat and their respective abundance (Shannon, 1948). All indices except mean year and mean latitude were calculated by the EwE (v.6.7.0) software (Christensen et al., 2005).

2.5 Estimation of ecological carrying capacity

The ecological carrying capacity (ECC) represents the maximum biomass of target species or functional groups that the ecosystem can sustain without significantly altering its primary energy flow or food web structure (Tang, 1996). Drawing on the literature applying EwE to analyze the ECC of aquatic ecosystems (Feng et al., 2025; Yan et al., 2025), these studies consistently adopt the approach of gradually increasing the biomass of target functional groups until the ecosystem becomes imbalanced. The critical point immediately preceding this imbalance is then defined as the ECC (Jiang and Gibbs, 2005). No parameters other than the biomass of the target functional group were manually altered during the calculation of the ECC. Therefore, the present study defines ECC as the trophic upper bound under steady-state assumptions, and was estimated by progressively increasing the biomass of each functional group until its *EE* the upper bound of 1.0, indicating that the total production demand equaled or exceeded the available system supply. The ECC estimated in this study is based on trophic constraints within a steady-state Ecopath model framework, and the underlying rationale is that *EE* represents the proportion of a functional group’s production that is utilized by predation, biomass accumulation, or exports. As *EE* approaches its upper bound of 1.0, total system demand equals available production, indicating that no surplus energy remains to support additional biomass. Under steady-state assumptions, further increases in biomass would therefore result in trophic imbalance.

The specific procedure for assessing ECC was as follows: after the model was fully balanced and validated, when measuring the ECC of a single target functional group, the biomass of that individual target functional group was incrementally increased by

10% per step until the *EE* of any functional group in the model reached the upper bound of 1.0. The biomass level achieved in the preceding step was then identified as the maximum ECC for that specific functional group. When measuring the ECC for all target functional groups collectively, the biomass of each target group was uniformly increased by 10% per step until the *EE* of any functional group in the model reached the upper bound of 1.0. The biomass level attained in the preceding step was then defined as the maximum ECC for all target functional groups as a whole. In the model, changes in the biomass of each functional group affect the energy dynamics of their prey and predators. Eight target functional groups of ecological and economic importance—large pelagic fishes, small pelagic fishes, large demersal fishes, medium demersal fishes, small demersal fishes, benthic crustaceans, small benthic invertebrates, and cephalopods—were selected for ECC estimation.

3 Results

3.1 Sampling results, PREBAL diagnostics and model balancing

All species collected through field surveys were assigned to functional groups 3–12, demersal fishes and benthic invertebrates accounted for the largest proportion of the observed biomass (Table 1). Their sampled biomass data were appropriately processed and subsequently directly input into the model as *in situ* measurements.

According to PREBAL diagnostics, WIMR biomass estimates span 6 orders of magnitude (biomass in an aquatic ecosystem typically covers 5–7 orders of magnitude (Link, 2010)). After log transformation, the biomass of each functional group generally follows the principle of decreasing with increasing trophic levels, with the slope of the trend line being -0.274 (a general range is -0.05 to -0.1 (Link, 2010)), WIMR ecosystem primary producers and functional groups of low TLs have significantly higher biomass than secondary consumers at high TLs. *P/B* and *Q/B* values for each functional group decrease with increased TL, and biomass and production values for each functional group of consumers also exceed those of primary producers. Total consumption removals for each consumer functional group are lower than production values (Supplementary Figure 1).

The Pedigree index of the Ecopath model for the WIMR ecosystem was 0.586, which was in line with expectations compared with the range (0.16–0.68) reported by Morissette et al. (2006) for 150 Ecopath models worldwide, the present model demonstrates satisfactory confidence in its parameterization.

3.2 Trophic level characteristics

The input and output parameters of the Ecopath model for the WIMR ecosystem are summarized in Table 2. The estimated ecotrophic efficiency (*EE*) values of the 17 functional groups ranged from 0.018 to 0.865. Cephalopods and pelagic fishes

TABLE 2 Basic input and output parameters of functional groups estimated by the Ecopath model for the ecosystem of Wailingding Island marine ranch, * is balanced data.

NO.	Functional group	TL	B (t/km ²)	P/B	Q/B	EE	P/Q	NE	R/B
1	Seabirds ^[1,2]	3.698	0.0024*	0.060	76.280	0.001 <	0.001	0.001	60.964
2	Marine mammals ^[1,2,4]	3.737	0.0090*	0.045	14.800	0.001 <	0.003	0.004	11.795
3	Cartilaginous fishes ^[1,2,4]	3.642	0.0025	0.450	6.800	0.255	0.066	0.083	4.990
4	Small benthic invertebrates ^[1-4]	2.164	3.4900	8.000	38.000	0.608	0.211	0.263	22.400
5	Benthic crustaceans ^[1-5]	2.425	4.6300	6.000	28.000	0.543	0.214	0.268	16.400
6	Cephalopods ^[1-4]	2.871	0.0075	3.010	12.000	0.865	0.251	0.314	6.590
7	Large pelagic fishes ^[1-4]	3.503	0.0173	1.310	6.350	0.852	0.206	0.258	3.770
8	Small pelagic fishes ^[1-4]	2.610	0.1430	2.880	11.500	0.752	0.250	0.313	6.320
9	Large demersal fishes ^[1-4]	2.828	0.0001	1.230	5.500	0.582	0.224	0.280	3.170
10	Medium demersal fishes ^[1-4]	2.742	0.1155	2.200	8.300	0.474	0.265	0.331	4.440
11	Small demersal fishes ^[1-4]	2.627	0.9270	3.000	12.000	0.599	0.250	0.313	6.600
12	Jellyfish ^[1,2,4]	2.533	1.6800	5.000	25.000	0.018	0.200	0.250	15.000
13	Zooplankton ^[1-4]	2.105	4.8825	55.000	186.000	0.536	0.296	0.370	93.800
14	Bacteria ^[4]	1.000	3.9715	32.000	–	0.729	–	–	–
15	Seaweeds ^[5,6]	1.000	10.7136	12.000	–	0.500	–	–	–
16	Phytoplankton ^[1-4]	1.000	22.6940	200.000*	–	0.116	–	–	–
17	Detritus ^[1-4]	1.000	7.5913	–	–	0.081	–	–	–

Values in bold were estimated by the model; TL, Trophic level; B: biomass; P/B: production/biomass; Q/B: consumption/biomass; EE: ecotrophic efficiency; P/Q: production/consumption; NE: net efficiency; R/B: respiration/biomass. Input parameters (except B) reference source: [1] (Liu et al., 2019b); [2] (Chen and Qiu, 2010); [3] (Feng et al., 2025); [4] (Sun et al., 2016); [5] (Liu et al., 2019a); [6] (Zhang et al., 2022).

exhibited the highest EE values (0.752–0.865), indicating efficient energy utilization and strong trophic linkages within the ecosystem.

For all groups except top predators, the production-to-consumption (P/Q) ratios ranged between 0.1 and 0.3, which is ecologically reasonable. The trophic levels (TLs) of the 17 functional

groups ranged from 1.000 to 3.737, encompassing three trophic layers. Marine mammals occupied the highest TL (3.737), followed by seabirds (3.698), while zooplankton exhibited the lowest (2.105).

The food web diagram (Figure 2) illustrates the trophic relationships, where circle sizes represent biomass magnitudes,

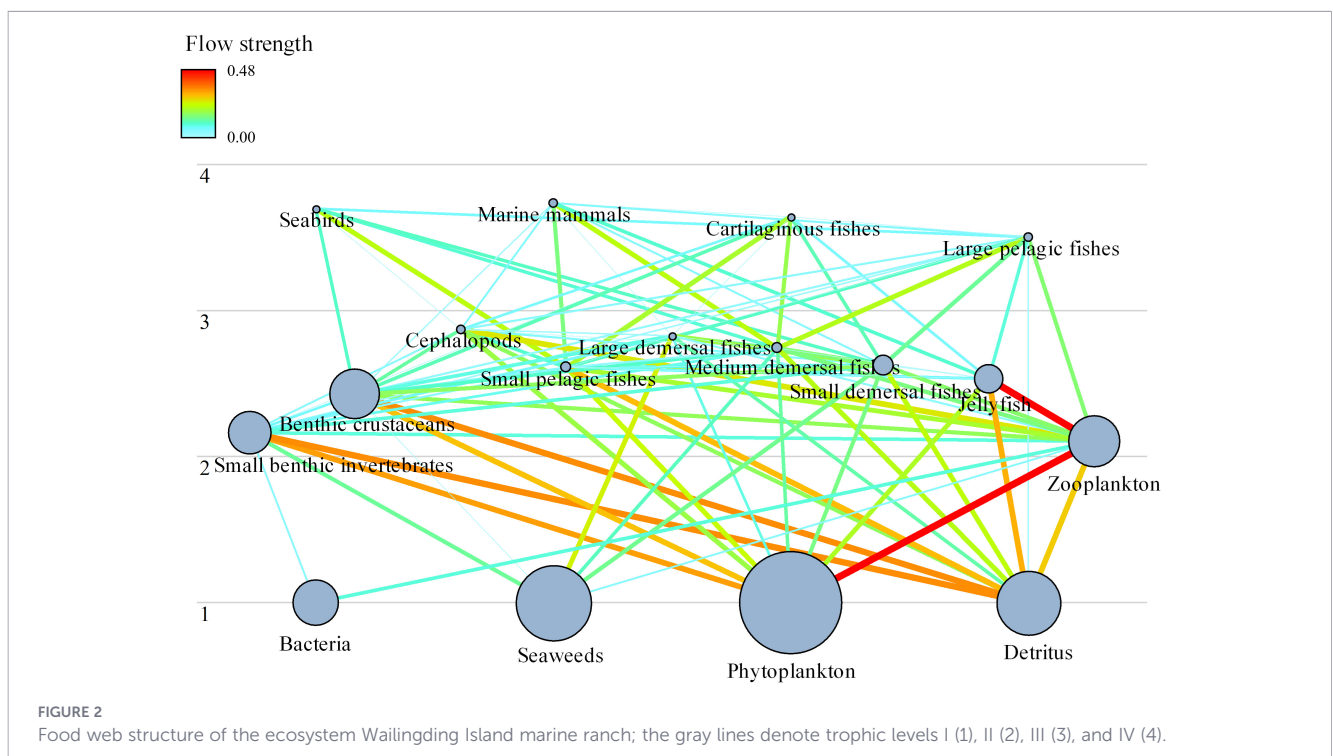


FIGURE 2 Food web structure of the ecosystem Wailingding Island marine ranch; the gray lines denote trophic levels I (1), II (2), III (3), and IV (4).

color gradients indicate dietary proportions, and link thickness denotes predation intensity. Under the current functional group aggregation and available data resolution, the modeled food web exhibits relatively short energy pathways and low apparent complexity.

3.3 Energy flow and transfer efficiency

Ecopath simulations revealed detailed energy transfer processes among TLs in the marine ranch ecosystem of Wailingding Island. Primary producers contributed a total production of 4,794.449 t/(km²·year), of which 682.100 t/(km²·year) (14.23%) was consumed by TL II organisms. Approximately 4,112 t/(km²·year) of primary production flowed into detritus, entering the recycling subsystem.

The total detrital input from all TLs was 4,515 t/(km²·year), of which only 366.1 t/(km²·year) (8.11%) was re-consumed by detritivores, while the remainder was lost through mineralization

and sedimentation. The proportions of total energy flow entering TL I, II, III, and IV were 45.98%, 10.05%, 0.653%, and 0.017%, respectively (Figure 3).

Energy aggregation by TL showed that total flow decreased sharply with increasing TL (Table 3). TLs I and II accounted for 89.28% and 10.05% of the total system flow, respectively, while TLs III and IV together contributed less than 1%.

The transfer efficiency between successive TLs indicated that energy transfer from primary producers to TL II was 6.666%, and from detritus to TL II was 6.170% (Table 4). The lowest transfer efficiency occurred between TLs II and III (approximately 2.5%).

Overall, the ecosystem exhibited a mean transfer efficiency of 3.873%, with similar contributions from the grazing (3.883%) and detrital (3.853%) pathways. Nearly half of the total system flow (49%) originated from detrital sources, underscoring the strong dependence of this estuarine system on detrital recycling.

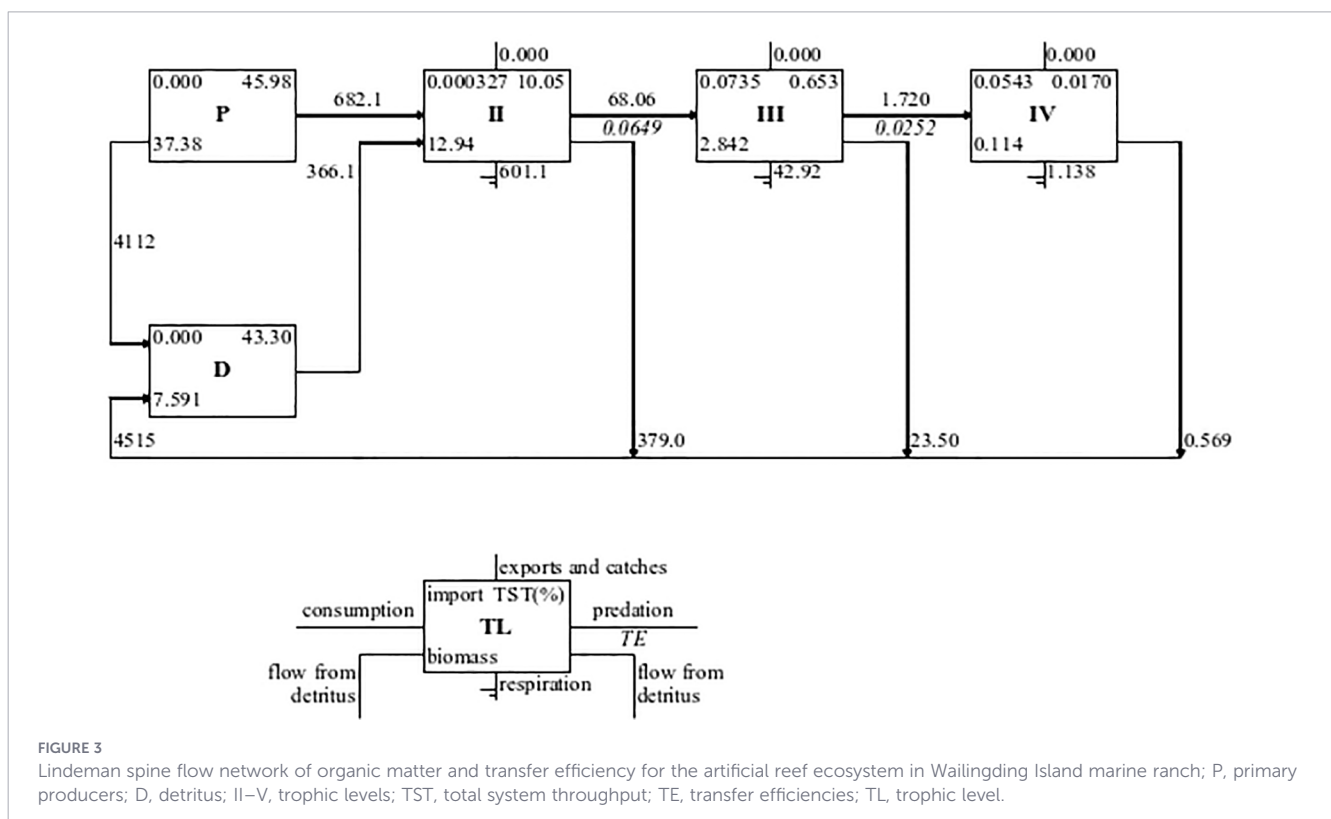


TABLE 3 Distribution of energy flow among trophic levels in the ecosystem of Wailingding Island marine ranch.

Trophic level	Consumption by predators	Export	Flow to detritus	Respiration	t/(km ² ·year) Throughput
IV	0.06	0.00	0.57	1.14	1.77
III	1.72	0.00	23.50	42.92	68.14
II	68.06	0.00	379.00	601.10	1,048.00
I	1,048.00	4,149.00	4,112.00	0.00	9,310.00
Sum	1,118.00	4,149.00	4,515.00	645.20	10,428.00

TABLE 4 Transfer efficiency among discrete trophic levels in the ecosystem of Wailingding Island marine ranch.

Source	Trophic level			%
	II	III	IV	
Producer	6.666	2.517	3.490	
Detritus	6.170	2.536	3.654	
All flows	6.493	2.523	3.545	
Proportion of total flow originating from detritus:49				
From primary producers:3.883				
From detritus:3.853				
Mean transfer efficiency:3.873				

3.4 Mixed trophic impact, keystone species and niche overlap

The mixed trophic impact analysis revealed the direct and indirect trophic relationships among functional groups; relative impact range between -1.0 and 1.0, and are comparable (Figure 4). Both detritus and primary producers exerted strong positive effects on most consumer groups. For instance, detritus exerts a positive influence on multiple functional groups, including benthic crustaceans, small benthic invertebrates, and small pelagic fishes, while seaweeds and phytoplankton enhanced the productivity of demersal fish groups.

In contrast, high-trophic-level predators exerted strong negative effects on their prey groups. An increase in prey biomass generally had a positive cascading effect on predators. Zooplankton, as primary consumers, showed pronounced negative impacts on

detritus and primary producers, highlighting their crucial role in energy transfer and bottom-up regulation.

The keystone species analysis (Figure 5) ranked functional groups by relative total impact and keystone index. The results identified small pelagic fishes and marine mammals as having the highest scores in both keystone index and relative total impact, followed by zooplankton. These groups serve as essential nodes in the food web, playing pivotal roles in maintaining ecosystem stability and energy flow dynamics. In contrast, large demersal fish emerged as the functional group with the lowest scores in both keystone index and relative total impact, which differed markedly from all other groups.

Overall, the trophic niche overlap between cartilaginous fishes and small pelagic fishes is the lowest, while small benthic invertebrates and benthic crustaceans have the most similar ecological overlap. Although the predator overlap index between small benthic invertebrates and zooplankton is relatively low, they have a relatively high prey overlap index, whereas cartilaginous fishes and large demersal fishes show the exact opposite pattern (Figure 6).

3.5 Estimation of ecological carrying capacity

Based on the economic value and ecological benefits of the species, and through expert consultation and practical experience, we identified eight target functional groups for the assessment of their respective ECC (Table 5). Under the current ecosystem conditions, large pelagic fishes exhibited the lowest ECC, reaching only 1.6 times their present biomass, whereas small pelagic fishes displayed a higher ECC of 8.5 times.

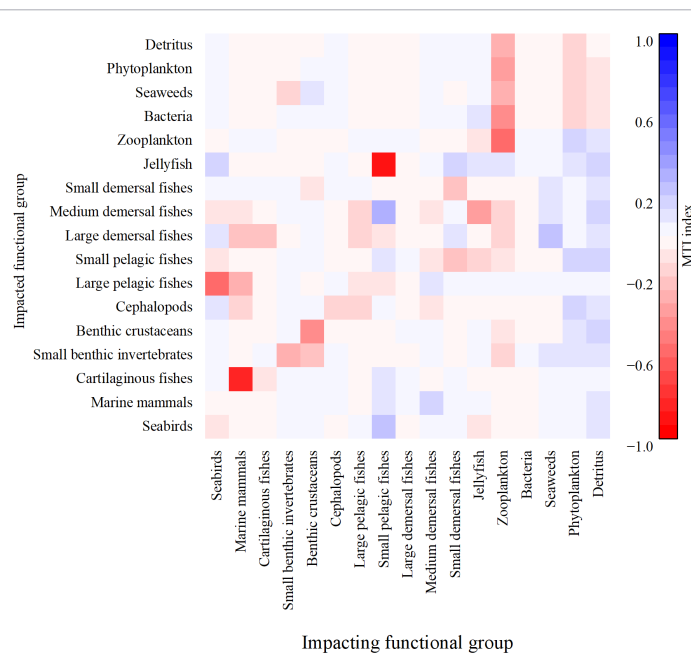


FIGURE 4 Mixed trophic impacts among functional groups in the ecosystem of Wailingding Island marine ranch. The matrix discriminates among positive (blue) and negative (red) overall effects.

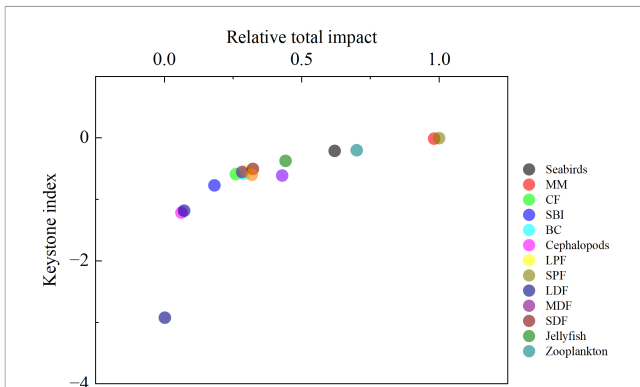


FIGURE 5 Keystone index for the functional groups of the ecosystem in Wailingding Island marine ranch; MM, marine mammals; CF, cartilaginous fishes; SBI, small benthic invertebrates; BC, benthic crustaceans; LPF, large pelagic fishes; SPF, small pelagic fishes; LDF, large demersal fishes; MDF, medium demersal fishes; SDF, small demersal fishes.

Among all groups, large demersal fishes demonstrated the greatest ECC, exceeding 100 times their current biomass, indicating substantial potential for population enhancement. Cephalopods also showed relatively high ECC values, up to 12 times their current biomass.

When all eight target groups were simultaneously increased, the ecosystem remained balanced until their combined biomass reached approximately 3.8 times the current level. Beyond this threshold, model instability occurred ($EE \geq 1$), indicating that the system had reached its upper ecological limit under existing environmental conditions.

3.6 Overall ecosystem characteristics

The Ecopath model outputs indicated that the total system throughput (TST) of WIMR ecosystem was 10,536.750 t/(km²·year).

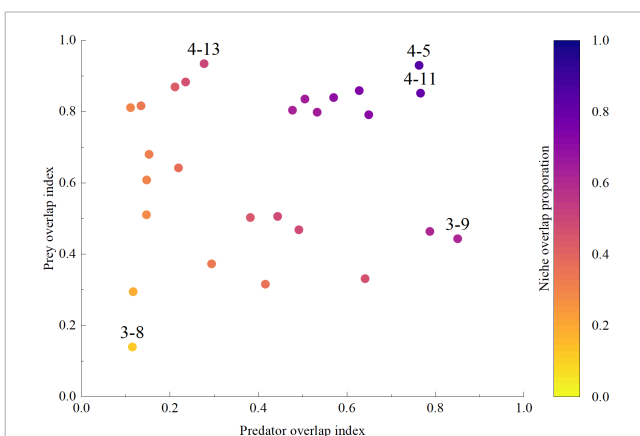


FIGURE 6 Trophic niche overlap plot of functional groups in Ecopath model (shows the degree to which different functional groups in WIMR ecosystem utilize the same food resources). Point colors represent geometric mean of “prey overlap index” and “predator overlap index” (color scale to right); functional groups: 3-8, cartilaginous fishes and small pelagic fishes; 4-13, small benthic invertebrates and zooplankton; 4-5, small benthic invertebrates and benthic crustaceans; 4-11, small benthic invertebrates and small demersal fishes; 3-9, cartilaginous fishes and large demersal fishes.

The total consumption (TC), total exports (TEx), total respiration (TR), and total flow to detritus (TFD) were 1,226.665, 4,149.389, 645.201, and 4,515.499 t/(km²·year), respectively, accounting for 11.64%, 39.38%, 6.12%, and 42.85% of TST .

When the biomasses of the eight target functional groups increased to their ECC levels, TST , TC , and TR rose to 11,500.840, 2,138.082, and 1,179.000 t/(km²·year), respectively. The TPP/TR ratio declined from 7.431 to 4.184, suggesting reduced excess primary production under expanded biomass scenarios. In contrast, Finn’s cycling index (FCI) and Finn’s mean path length (FML) slightly increased, implying modest improvement in system maturity and energy recycling. In addition, the model calculated Shannon diversity index and mTE values rose from 1.704 to 1.856 and 3.873% to 4.801%, respectively, which demonstrate that an appropriate increase in the biomass of target functional groups can play a certain role in improving the overall state of the ecosystem (Table 6).

4 Discussion

4.1 Summary statistics, trophic structure and energy flows

In the present study we describe the structure and functioning of the ecosystem of WIMR. Our estimate of the total fish biomass (1.21 t/km²) was slightly higher than what has been reported before for the marine ranch in the Beibu Gulf (1.13 t/km²) (Feng et al., 2025), indicating that our survey results are generally consistent with those of adjacent seas at the same latitude. However, it was significantly lower than that reported for temperate artificial reef areas in the Bohai Sea (9.01 t/km²) (Yan et al., 2025) and the Yellow Sea (5.89 t/km²) (Zhang et al., 2022). This deviation could be explained by environmental differences across the latitudinal gradient, as well as by the higher density of artificial reefs.

The WIMR ecosystem was dominated by lower trophic levels (TLs), with TL I and TL II contributing 89.28% and 10.05% of the total system throughput (TST), respectively. In this ecosystem, the contribution of detritus to the TST substantially exceeds that reported for artificial reef ecosystems in the Beibu Gulf (Feng et al., 2025) and the northern Yellow Sea (Zhang et al., 2022). Biomass distribution followed a similar pattern, with 73.87% of total biomass concentrated in TL I and 26.08% in TL II. Most of the energy produced by primary producers flowed into detritus, accounting for 91.07% of total detrital input, whereas only 8.11% was re-consumed by the food web. In stark contrast, the proportion of primary production flowing back to detritus reported in studies of artificial reefs in coastal waters of the Beibu Gulf at similar latitudes and the northern Yellow Sea at higher latitudes ranges from 30 to 50% (Zhang et al., 2022; Feng et al., 2025). The pattern of the WIMR ecosystem indicates that a large fraction of primary productivity was not efficiently transferred to consumers, instead accumulating as organic detritus at lower TLs. The limited recycling rate restricted the re-entry of detrital energy into higher trophic pathways, implying inefficient utilization of primary production within the ecosystem.

TABLE 5 Maximum ecological carrying capacities of target functional groups in the ecosystem of the National marine ranch demonstration zone of Wailingding Island.

Functional group	Current biomass (t/km ²)	Biomass multiples to reach ECC (100%)
Small benthic invertebrates	3.4900	6.5
Benthic crustaceans	4.6300	2.2
Cephalopods	0.0075	12.0
Large pelagic fishes	0.0173	1.6
Small pelagic fishes	0.1430	8.5
Large demersal fishes	0.0001	>100
Medium demersal fishes	0.1155	3.5
Small demersal fishes	0.9270	2.0

Furthermore, the mean transfer efficiency (mTE, 3.873%) of the WIRM ecosystem was lower than the theoretical reference value of approximately 10% commonly reported for aquatic ecosystems (Lindeman, 1942), suggesting relatively low energy transfer efficiency and limited internal cycling in the modeled ecosystem. The mTE estimated in this study is relatively low compared with values reported for highly resolved or fishery-inclusive Ecopath models, the mTE values reported for coastal Ecopath models with comparable aggregation levels typically range from approximately 6.0 to 10.0% (Wang et al., 2022a; Zhang et al., 2022; Feng et al., 2025; Yan et al., 2025). However, mTE is known to be sensitive to model structure, particularly the level of functional group aggregation and the representation of detrital pathways. In addition, the absence of explicit fishing activity in the model may

TABLE 6 Total system properties of the artificial reef ecosystem in the National marine ranch demonstration zone of Wailingding Island.

Parameter	Value	Value*	Units
Total system throughput (TST)	10,536.750	11,500.840	t/(km ² ·year)
Total consumption (TC)	1,226.665	2,138.082	t/(km ² ·year)
Total exports (TE _x)	4,149.389	3,754.487	t/(km ² ·year)
Total respiratory flows (TR)	645.201	1,179.000	t/(km ² ·year)
Total flow into detritus (TFD)	4,515.499	4,429.276	t/(km ² ·year)
Total primary production (TPP)	4,794.449	4,933.290	t/(km ² ·year)
Total biomass (excluding detritus) (TB)	53.286	95.646	t/(km ² ·year)
TPP/TR	7.431	4.184	–
TPP/TB	89.976	51.579	–
TB/TST	0.005	0.008	–
Finn's cycling index (FCI)	2.529	3.687	%
Finn's mean path length (FML)	2.198	2.331	–
Shannon diversity index	1.704	1.856	–
Mean transfer efficiency (mTE)	3.873	4.801	%

*"–" indicates system parameters when the eight target functional groups reached their ecological carrying capacities.

further reduce apparent transfer efficiency to higher trophic levels. Reduced TE has frequently been documented in estuarine and coastal ecosystems characterized by high detrital inputs and strong internal recycling (Sobczak et al., 2005; Lobry et al., 2008; Valentine et al., 2014). In the present study, although the highest transfer efficiency occurred between TL I and TL II, highlighting the critical role of primary consumers in channeling energy upward through the food web, a substantial proportion of primary production was routed into detrital pathways, limiting direct energy transfer to higher trophic levels. Additionally, high respiration losses at lower trophic levels further constrained the amount of energy available for upward transfer, a mechanism widely recognized in Ecopath-based analyses of coastal ecosystems (Abdul and Adekoya, 2016; Yuan et al., 2024; Wenhui et al., 2025).

Some functional groups exhibited relatively low EE values, particularly zooplankton and jellyfish. Low EE values do not necessarily indicate model deficiencies, but rather reflect weak predation pressure and inefficient transfer of production to higher trophic levels, a pattern commonly reported in eutrophic coastal and estuarine ecosystems (Pauly et al., 2000; Lobry et al., 2008). In such ecosystems, a substantial fraction of production is dissipated through respiration and natural mortality rather than being incorporated into higher trophic pathways. In coastal ecosystems, jellyfish primarily consume mesozooplankton but are also known to feed opportunistically on microzooplankton, fish eggs and larvae, and suspended particulate organic matter, all of which occupy low trophic positions (Purcell, 2003; Pitt et al., 2009). This is particularly relevant considering the frequent reports of jellyfish outbreaks in the coastal waters of the northern South China Sea (Du et al., 2022). The massive aggregation of jellyfish may exert a negative impact on zooplankton, yet it likely fails to effectively transfer energy to higher TLs, implying a weak trophic coupling between jellyfish and the upper trophic layers in coastal ecosystems (Wang et al., 2024a). Therefore, this study shows that jellyfish channel primary production into pathways with poor transfer efficiency rather than supporting higher trophic levels within the WIMR ecosystem, reflecting weak top-down control and limited utilization by predators.

Overall, the low trophic transfer efficiency observed in the WIMR ecosystem reflects two primary ecological constraints. On the one hand, excessive nutrient inputs from terrestrial runoff and anthropogenic activities have led to frequent harmful algal blooms (Yao and Chen, 2021), and primary production likely exceeds the consumption capacity of higher trophic levels. This unbalanced input of primary productivity hampers effective energy transfer and constrains the development of a mature and well-structured food web (Cloern et al., 2014). On the other hand, long-term fishing pressure and environmental pollution in the Pearl River Estuary have contributed to declines in high-trophic-level species, simplification of the fish community, and a shift toward smaller, lower-value species (Jackson et al., 2001; Pauly and Palomares, 2005). Although the Ecopath model in this study did not explicitly include fishing due to the location of the study area within a no-fishing zone, previous studies have shown that fishing pressure can influence trophic interactions and energy transfer efficiency in adjacent marine ecosystems (Binch et al., 2025). The loss of apex

predators and degradation of habitat complexity weaken trophic regulation, disrupt energy transfer pathways, and reduce overall ecosystem resilience (Folke et al., 2004; Myers et al., 2007; Hughes et al., 2024). Consequently, in light of our simulation results showing an increase in mTE from augmenting the biomass of target functional groups, it is crucial to strengthen resource conservation and ecological restoration (such as habitat rehabilitation (Tanaya et al., 2025) and reductions in nutrient input) to improve trophic transfer efficiency and enhancing the resilience of the ecosystem to both natural and anthropogenic disturbances (Folke et al., 2004; Pauly and Palomares, 2005).

4.2 Food web dynamic analysis

Mixed trophic impact (MTI) analysis provides insight into the direct and indirect interactions among functional groups and has been widely applied to identify ecosystem regulation mechanisms in marine food webs (Christensen and Walters, 2004). Although most functional groups showed that a slight change in biomass would have a low and negligible impact on others, benthic invertebrates displayed positive impacts on demersal fishes, underscoring the importance of benthic–pelagic coupling in sustaining higher trophic levels, as reported in other marine ecosystems (Griffiths et al., 2017; Ehrnsten et al., 2019; Searles et al., 2022).

In addition, keystone index analysis reveals pronounced differences in the functional importance of trophic groups within the ecosystem. Functional groups at mid- or lower-trophic levels exhibited the highest keystone index values, indicating a disproportionate influence on trophic structure and energy flow relative to their biomass (Jordán, 2009). The particularly high ranking of zooplankton as a keystone group also underscores the importance of bottom-up processes in regulating ecosystem stability. Libralato et al. (2006) demonstrated that in many coastal ecosystems, low-trophic-level species such as zooplankton often exhibit high keystone indices, indicating their critical role in mediating energy transfer across TLs. Thus, the low trophic position of zooplankton act as key functional drivers of stability and productivity in the WIMR ecosystem (Lomartire et al., 2021). The negative self-impact observed for zooplankton in the MTI analysis does not indicate a modeling error or internal inconsistency. In Ecopath model, self-effects can arise from indirect feedback mechanisms, including density-dependent processes and detritus-mediated pathways. In the present model, zooplankton consume both phytoplankton and detritus, and an increase in zooplankton biomass enhances competition for shared resources while simultaneously increasing detrital recycling demands. In contrast, higher trophic predators showed relatively low keystone index values, suggesting weakened top-down control under current ecosystem conditions. Similar shifts in keystone roles from apex predators to mid-trophic-level groups have been widely reported in marine ecosystems, where sustained fishing pressure and habitat modification reduce predator regulation capacity (Pauly and Palomares, 2005). This pattern highlights the importance of functional connectivity mediated by intermediate trophic groups in maintaining ecosystem stability.

Furthermore, The niche overlap index mainly describes niche partitioning between functional groups; it is based on similarities in, for example, predation, competition, and environmental adaptation (Pianka, 1973). The observed patterns of trophic niche overlap further elucidate the mechanisms underlying ecosystem regulation in the WIMR system. The lowest trophic niche overlap between cartilaginous fishes and small pelagic fishes suggests a high degree of trophic differentiation, indicating limited competition for food resources and distinct ecological roles within the food web (Finotto et al., 2023; Ruzicka et al., 2024). In contrast, the high niche overlap between small benthic invertebrates and benthic crustaceans reflects their similar feeding strategies and shared reliance on benthic and detrital energy pathways, a pattern commonly reported in benthic-dominated marine ecosystems (Krumhansl and Scheibling, 2012). Notably, although the predator overlap index between small benthic invertebrates and zooplankton is relatively low, their high prey overlap index indicates convergence in resource utilization at lower trophic levels. This pattern suggests that these groups contribute to parallel energy pathways that support higher trophic levels, reinforcing bottom-up control within the ecosystem (Ware and Thomson, 2005). In contrast, cartilaginous fishes and large demersal fishes exhibit low prey overlap but relatively high predator overlap, implying shared predation pressures rather than direct competition for resources. Such a pattern is characteristic of systems with reduced apex predator regulation, where higher trophic groups respond similarly to changes in prey availability but exert limited differential control over lower trophic levels (Frank et al., 2005; Myers et al., 2007).

Overall, these niche overlap patterns complement the MTI results by highlighting the dominant role of benthic and lower trophic groups in structuring energy flow and trophic interactions in the WIMR ecosystem. The combination of high overlap among benthic consumers and weak trophic coupling at higher levels further supports the conclusion that ecosystem functioning is primarily governed by bottom-up processes, with limited top-down regulation shaping food-web dynamics (Ware and Thomson, 2005; Lynam et al., 2017). In this context, from a management perspective, ecological restoration and marine ranch development should prioritize maintaining trophic balance and functional connectivity across trophic levels, rather than maximizing biomass of selected species. Such an approach aligns with ecosystem-based management principles and provides a more robust foundation for rebuilding stable, resilient, and energetically efficient food webs in marine ranching ecosystems (Pikitch et al., 2004; Levin et al., 2009).

4.3 Ecosystem maturity and stability

Ecosystem-level indices derived from the Ecopath model provide valuable indicators of system maturity and developmental state. In the absence of external disturbances, ecosystems typically evolve toward greater structural complexity, higher recycling efficiency, and improved stability (Lobry et al., 2008; Rahman et al., 2019).

In this study, the TPP/TR ratio (7.431) was substantially greater than unity, suggesting that the marine ranch ecosystem of Wailingding Island remains in an early developmental stage, with a large portion of primary production unutilized by consumers (Abdul and Adekoya, 2016). The low Finn's cycling index (FCI = 2.529%) and Finn's mean path length (FML = 2.198) demonstrate limited energy recycling and short trophic chains in the simulated WIMR ecosystem (Abdul and Adekoya, 2016). Collectively, these metrics confirm that the ecosystem exhibits low maturity, low resilience, and limited self-regulatory capacity, the ecosystem may remain in a transitional and structurally simplified state.

Such structural and functional features are consistent with the long-term ecological pressures documented in the Pearl River Estuary, including nutrient enrichment, overexploitation of living resources, and habitat modification (Zeng et al., 2022). These stressors tend to disrupt trophic connectivity, truncate food chains, and impair energy transfer efficiency, ultimately constraining ecosystem development and stability (Zhang et al., 2025). From a management standpoint, the convergence between modeled trophic structure and documented anthropogenic stressors suggests that the current ecosystem configuration may represent a stress-mediated state rather than a fully developed or mature food web. Consequently, efforts to enhance ecosystem maturity in marine ranching areas should not only aim to increase biomass or production, but also to restore trophic connectivity and improve energy transfer efficiency. This may involve coordinated measures that reduce nutrient-driven imbalances, regulate fishing pressure to prevent further trophic truncation, and restore benthic habitats that support energy recycling pathways (Christensen and Walters, 2004; Pikitch et al., 2004; Levin et al., 2009). By explicitly addressing the structural constraints revealed by the model, such integrated strategies are more likely to promote long-term ecosystem stability and resilience than isolated or species-specific interventions. Accordingly, in the context of integrated marine fisheries management for the Pearl River Estuary, enhancing ecosystem maturity will require multiple measures, including habitat restoration, sustainable fisheries regulation, and effective pollution mitigation (Wang et al., 2016).

4.4 Ecological carrying capacity and management implications

Changes in ecosystem-level indicators under the ECC scenario provide important insights into how biomass enhancement influences ecosystem functioning and structural organization in the WIMR. It is important to emphasize that rather than representing the equilibrium biomass emerging from temporal dynamics, the ECC estimated in this study reflects a trophic constraint-based upper bound derived under steady-state assumptions, where EE approaches its theoretical maximum. As such, ECC should be interpreted as an energy-limited ceiling imposed by food-web structure rather than a predictive estimate of long-term sustainable biomass. At the original state, the ecosystem was characterized by a high TST, with a substantial proportion of flows directed toward detritus and exports, indicating strong dissipation of energy and weak retention within internal

trophic pathways (Odum, 1969). Such a flow structure reflects a system with limited recycling efficiency and a relatively low degree of trophic integration (Finn, 1976; Lobry et al., 2008).

Model simulations under increasing ecological capacity further reveal how structural constraints shape ecosystem responses to biomass enhancement. ECC analysis indicates that the potential for biomass enhancement varies substantially among functional groups and is strongly constrained by underlying trophic structure and energy availability (Christensen and Pauly, 1998). In the present study, Large pelagic fishes exhibited the lowest ECC, whereas large demersal fishes displayed the highest, exceeding 100 times their current biomass. This contrast suggests that energy flow within the existing food web can more effectively support demersal production than pelagic biomass expansion (Shi et al., 2024). The low ECC of large pelagic fishes indicates that the ecosystem currently lacks sufficient trophic support and energy transfer efficiency to sustain high-level predators (Heymans et al., 2016). In contrast, the abundant benthic productivity provides favorable conditions for demersal species enhancement (Pauly and Christensen, 1995). Similar findings have been reported in previous Ecopath model studies, where increases in higher trophic levels were limited by low energy transfer efficiency and reduced trophic connectivity (Christensen and Pauly, 1998; Salomon et al., 2002). The deviation between observed biomass and ECC reflects the degree of trophic linkage or structural constraint within the system. Functional groups with biomass values close to ECC may operate near energetic limits and thus be more sensitive to perturbations, whereas large deviations may indicate structural bottlenecks or unused production potential constrained by other ecological processes. The finding that higher trophic level predators are relatively closer to their ECC than lower trophic groups may instead reflect energy-limited compression at upper trophic levels, a common feature of ecosystems subjected to long-term anthropogenic pressure (Burdon et al., 2019; Mor et al., 2021). From a management perspective, these results suggest that stock enhancement or species-specific management strategies alone may be insufficient to improve ecosystem functioning without concurrent improvements in ecosystem structure and energy flow (Christensen and Walters, 2011). Effective ecosystem improvement thus requires consideration of structural food-web organization rather than reliance solely on stock enhancement measures.

In addition, when the biomasses of the eight target functional groups were increased to their ECC levels, TST, total consumption, and total respiration all increased markedly, indicating enhanced biological activity and intensified energy processing within the system (Salomon et al., 2002; Heymans et al., 2016). Concurrently, the decline in the TPP/TR ratio suggests a reduction in excess primary production, implying improved coupling between primary producers and consumers as biomass increased (Odum, 1969; Christensen, 1995). These changes indicate that moderate biomass enhancement can partially alleviate energy underutilization and promote more efficient transfer of energy to higher trophic levels. Consistent with this interpretation, modest increases in Finn's cycling index and Finn's mean path length under the ECC scenario indicate a slight enhancement in internal energy recycling and trophic pathway length, reflecting incremental

progress toward greater ecosystem maturity (Finn, 1976; Valentine et al., 2014). Similarly, increases in the Shannon diversity index and mTE further suggest that biomass enhancement contributes to improved functional diversity and energy utilization efficiency (Heymans et al., 2016), supporting short-term functional improvements in overall ecosystem condition (Duarte et al., 2008).

Taken together, these results indicate that while increasing the biomass of target functional groups can improve certain functional attributes of the ecosystem—such as energy utilization efficiency, diversity, and recycling—it is insufficient to fundamentally restructure the food web or substantially enhance ecosystem maturity (Odum, 1969; Libralato et al., 2006). From a management perspective, this finding highlights the limitations of relying solely on stock enhancement to achieve long-term ecosystem recovery. Effective management of the WIMR ecosystem should therefore adopt an ecosystem-based approach that combines biomass enhancement with measures aimed at reducing nutrient inputs, restoring benthic habitats, and strengthening trophic linkages across multiple levels (Pauly et al., 1998; Jackson et al., 2001; Halpern et al., 2008; Fulton et al., 2010). Such integrated strategies are essential to overcoming structural constraints and enhancing ecosystem resilience and sustainability at or near ecological carrying capacity (FAO, 2025).

As the eight target functional groups approached their ECC upper limit, both the Shannon diversity index and mean trophic transfer efficiency (mTE) increased, indicating that moderate increases in the biomass of target functional groups can partially enhance ecosystem diversity and improve the efficiency of energy transfer across trophic levels (Odum, 1969; Libralato et al., 2008; Heymans et al., 2016). These changes suggest that stock enhancement and biomass recovery measures may contribute to short-term functional improvements in ecosystem performance (Pauly and Christensen, 1995; Coll et al., 2006). The *TPP/TR* ratio decreased markedly, reflecting a more balanced metabolic state, and the FCI and FML increased, signifying enhanced internal energy recycling and improved system maturity. However, it should be noted that validation of Ecopath models differs from that of predictive dynamic models. The present model is best interpreted as a data-informed, steady-state representation of trophic structure constrained by mass balance and ecological plausibility, rather than as a predictive or forecast model. While this approach does not provide direct empirical validation in a strict statistical sense, it represents a widely accepted framework for exploring ecosystem organization and energy flows when dynamic data are limited.

Overall, the WIMR ecosystem exhibits low maturity, weak trophic connectivity, and limited energy recycling. An integrated approach—encompassing artificial reef deployment, habitat restoration, and scientifically guided stock enhancement—should therefore prioritize improving basal resource conditions and environment quality (Wang et al., 2024c). This foundational focus will underpin the restoration process, promoting more efficient energy transfer (Huang et al., 2019), enhancing resilience to environmental variability (Hughes et al., 2005; Folke et al., 2010),

and ultimately supporting the sustainable management of coastal fishery resources in the Pearl River Estuary.

5 Conclusion

This study applied an Ecopath modeling framework to evaluate the trophic structure, energy flow, and ecological carrying capacity of the National Wailingding Island Marine Ranch Demonstration Zone in the Pearl River Estuary. The results indicate a food web dominated by detrital and lower-trophic-level energy pathways, with low trophic transfer efficiency and limited regulation by higher trophic levels. Keystone index, mixed trophic impact, and niche overlap analyses consistently highlight the ecological importance of mid- and lower-trophic-level functional groups, while the influence of top predators remains relatively weak under current conditions. This ecosystem was predominantly regulated by bottom-up processes, with top-down control remaining limited, which reflects an early stage of ecosystem development despite ongoing habitat enhancement. The ecological carrying capacity analysis suggests that, although certain functional groups exhibit substantial potential for biomass enhancement, increases in stock abundance are constrained by existing trophic relationships and energy transfer efficiency. These findings highlight that marine ranch management in estuarine environments should prioritize ecosystem-level regulation rather than focusing solely on single-species enhancement. In particular, management strategies that promote multi-trophic balance, improve benthic–pelagic coupling, and reduce external disturbances such as excessive fishing pressure are likely to be more effective in enhancing ecosystem stability and sustainability.

Overall, this study provides a quantitative, ecosystem-based perspective on the functioning of a subtropical estuarine marine ranch and offers scientific support for adaptive management in the Pearl River Estuary. However, it should be noted that benthic functional groups accounted for a large proportion of total ecosystem biomass in the present model, the structure of the Ecopath model influences the magnitude and interpretation of ecosystem-level indicators. This configuration inherently emphasizes benthic and lower-trophic-level pathways and may contribute to relatively low estimates of trophic transfer efficiency and cycling indices. Due to limitations in data collection and processing methods, the characterization of the ecosystem in the study area remains incomplete. Future work should integrate additional sampling methods and scenario-based simulations to more realistically evaluate the long-term responses of the ecosystem to restoration and management measures.

Data availability statement

The original contributions presented in the study are included in the article/[Supplementary Material](#). Further inquiries can be directed to the corresponding author/s.

Ethics statement

The manuscript presents research on animals that do not require ethical approval for their study.

Author contributions

XF: Conceptualization, Data curation, Investigation, Writing – original draft. XH: Data curation, Formal analysis, Methodology, Software, Writing – original draft. PC: Funding acquisition, Writing – review & editing. JF: Project administration, Resources, Supervision, Validation, Visualization, Writing – review & editing.

Funding

The author(s) declared that financial support was received for this work and/or its publication. This study was supported by the following funds: (1) Research on Industrial Innovation Technology for Guangdong Modern Marine Ranching (2024-MRI-001); (2) Key-Area Research and Development Program of Guangdong Province, China (2020B1111030002); (3) Central Public-interest Scientific Institution Basal Research Fund, CAFS (2023TD06).

Acknowledgments

We thank all those involved in the marine surveys that collected the data used in this study.

References

- Abdul, W., and Adekoya, E. (2016). Preliminary Ecopath model of a tropical coastal estuarine ecosystem around bight of Benin, Nigeria. *Environ. Biol. Fishes* 99, 909–923. doi: 10.1007/s10641-016-0532-7
- Bentley, J. W., Chagaris, D., Coll, M., Heymans, J. J., Serpetti, N., Walters, C. J., et al. (2024). Calibrating ecosystem models to support ecosystem-based management of marine systems. *ICES J. Mar. Sci.* 81, 260–275. doi: 10.1093/icesjms/fsad213
- Binch, L., Poos, J. J., and van de Wolfshaar, K. (2025). Fishing effort displacement drives ecosystem impacts within and beyond marine protected areas. *Ecol. Model.* 510. doi: 10.1016/j.ecolmodel.2025.111336
- Burdon, F. J., McIntosh, A. R., Harding, J. S., and O’Gorman, E. (2019). Mechanisms of trophic niche compression: Evidence from landscape disturbance. *J. Anim. Ecol.* 89, 730–744. doi: 10.1111/1365-2656.13142
- Chen, K., Zhang, X., Liu, X., Huang, H., Xu, H., Shi, W., et al. (2020). Status and development trends of marine ranching in China. *Fishery Inf. Strategy* 35, 12–21. doi: 10.13233/j.cnki.fishis.2020.01.003
- Chen, Z., and Qiu, Y. (2010). Assessment of the food-web structure, energy flows, and system attribute of northern South China Sea ecosystem. *Acta Ecologica Sin.* 30, 4855–4865. doi: 10.20103/j.stxb.2010.18.005
- Christensen, V. (1995). Ecosystem maturity - towards quantification. *Ecol. Model.* 77, 3–32. doi: 10.1016/0304-3800(93)E0073-C
- Christensen, V., and Pauly, D. (1992). ECOPATH II — a software for balancing steady-state ecosystem models and calculating network characteristics. *Ecol. Model.* 61, 169–185. doi: 10.1016/0304-3800(92)90016-8
- Christensen, V., and Pauly, D. (1998). Changes in models of aquatic ecosystems approaching carrying capacity. *Ecol. Appl.* 8, S104–S109. doi: 10.2307/2641367
- Christensen, V., and Walters, C. J. (2004). Ecopath with Ecosim: methods, capabilities and limitations. *Ecol. Model.* 172, 109–139. doi: 10.1016/j.ecolmodel.2003.09.003
- Christensen, V., and Walters, C. J. (2011). “Progress in the use of ecosystem modeling for fisheries management,” in *Ecosystem approaches to fisheries: A global perspective*. Eds. V. Christensen and J. Maclean (Cambridge University Press, Cambridge), 189–206.
- Christensen, V., Walters, C. J., and Pauly, D. (2005). Ecopath with Ecosim: a user’s guide. *Fisheries Centre Univ. Br. Columbia Vancouver* 154.
- Christensen, V., Walters, C., Pauly, D., and Forrest, R. (2008). Ecopath with Ecosim version 6 user guide. *Lenfest Ocean Futures Project* 235.
- Cloern, J. E., Foster, S. Q., and Kleckner, A. E. (2014). Phytoplankton primary production in the world’s estuarine-coastal ecosystems. *Biogeosciences* 11, 2477–2501. doi: 10.5194/bg-11-2477-2014
- Coll, M., Palomera, I., Tudela, S., and Sardà, F. (2006). Trophic flows, ecosystem structure and fishing impacts in the South Catalan Sea, Northwestern Mediterranean. *J. Mar. Syst.* 59, 63–96. doi: 10.1016/j.jmarsys.2005.09.001
- Colléter, M., Valls, A., Guitton, J., Morissette, L., Arreguín-Sánchez, F., Christensen, V., et al. (2013). EcoBasE: a repository solution to gather and communicate information from EwE models. *Fisheries Centre Res. Rep.* 21, 60pp.
- Craig, J. K., and Link, J. S. (2023). It is past time to use ecosystem models tactically to support ecosystem-based fisheries management: Case studies using Ecopath with

Conflict of interest

The author(s) declared that this work was conducted in the absence of any commercial or financial relationships that could be construed as a potential conflict of interest.

Generative AI statement

The author(s) declared that generative AI was not used in the creation of this manuscript.

Any alternative text (alt text) provided alongside figures in this article has been generated by Frontiers with the support of artificial intelligence and reasonable efforts have been made to ensure accuracy, including review by the authors wherever possible. If you identify any issues, please contact us.

Publisher’s note

All claims expressed in this article are solely those of the authors and do not necessarily represent those of their affiliated organizations, or those of the publisher, the editors and the reviewers. Any product that may be evaluated in this article, or claim that may be made by its manufacturer, is not guaranteed or endorsed by the publisher.

Supplementary material

The Supplementary Material for this article can be found online at: <https://www.frontiersin.org/articles/10.3389/fmars.2026.1744551/full#supplementary-material>

- Ecosim in an operational management context. *Fish Fisheries* 24, 381–406. doi: 10.1111/faf.12733
- de Mutsert, K., Lewis, K. A., White, E. D., and Buszowski, J. (2021). End-to-end modeling reveals species-specific effects of large-scale coastal restoration on living resources facing climate change. *Front. Mar. Sci.* 8. doi: 10.3389/fmars.2021.624532
- Du, C., He, J., Sun, T., Wang, L., Wang, F., and Dong, Z. (2022). Molecular identification on the causative species jellyfish blooms in the northern South China Sea in 2019. *J. Trop. Oceanography* 41, 142–148. doi: 10.11978/2021071
- Duarte, C. M., Conley, D. J., Carstensen, J., and Sánchez-Camacho, M. (2008). Return to neverland: shifting baselines affect eutrophication restoration targets. *Estuaries Coasts* 32, 29–36. doi: 10.1007/s12237-008-9111-2
- Ehrnsten, E., Norkko, A., Timmermann, K., and Gustafsson, B. G. (2019). Benthic-pelagic coupling in coastal seas – Modelling macrofaunal biomass and carbon processing in response to organic matter supply. *J. Mar. Syst.* 196, 36–47. doi: 10.1016/j.jmarsys.2019.04.003
- FAO (2025). *The state of food and agriculture 2025*. (Rome, Italy: FAO).
- Feng, X., Fan, J., Sun, X., Hong, J., and Chen, P. (2021). The stock enhancement effect evaluation of artificial reef in Wailingding, Zhuhai. *J. South. Agric.* 52, 3228–3236. doi: 10.3969/j.issn.2095-1191.2021.12.005
- Feng, J., Yu, H., Wu, L., Yuan, C., Zhao, X., Sun, H., et al. (2025). Evaluating ecosystem characteristics and ecological carrying capacity for marine fauna stock enhancement within a marine ranching system. *Animals* 15. doi: 10.3390/ani15020165
- Finn, J. T. (1976). Measures of ecosystem structure and function derived from analysis of flows. *J. Theor. Biol.* 56, 363–380. doi: 10.1016/S0022-5193(76)80080-X
- Finotto, L., Berto, D., Rampazzo, F., Raicevich, S., Bonanomi, S., and Mazzoldi, C. (2023). Trophic partitioning among three mesopredatory shark species inhabiting the northwestern adriatic sea. *Diversity* 15. doi: 10.3390/d15121163
- Folke, C., Carpenter, S. R., Walker, B., Scheffer, M., Chapin, T., and Rockström, J. (2010). Resilience thinking: integrating resilience, adaptability and transformability. *Ecol. Soc.* 15. doi: 10.5751/ES-03610-150420
- Folke, C., Carpenter, S., Walker, B., Scheffer, M., Elmqvist, T., Gunderson, L., et al. (2004). Regime shifts, resilience, and biodiversity in ecosystem management. *Annu. Rev. Ecology Evolution Systematics* 35, 557–581. doi: 10.1146/annurev.ecolsys.35.021103.105711
- Frank, K. T., Petrie, B., Choi, J. S., and Leggett, W. C. (2005). Trophic cascades in a formerly cod-dominated ecosystem. *Science* 308, 1621–1623. doi: 10.1126/science.1113075
- Fulton, E. A., Smith, A. D. M., Smith, D. C., and van Putten, I. E. (2010). Human behaviour: the key source of uncertainty in fisheries management. *Fish Fisheries* 12, 2–17. doi: 10.1111/j.1467-2979.2010.00371.x
- Griffiths, J. R., Kadin, M., Nascimento, F. J. A., Tamelander, T., Törnroos, A., Bonaglia, S., et al. (2017). The importance of benthic-pelagic coupling for marine ecosystem functioning in a changing world. *Global Change Biol.* 23, 2179–2196. doi: 10.1111/gcb.13642
- Halpern, B. S., Walbridge, S., Selkoe, K. A., Kappel, C. V., Micheli, F., D'Agrosa, C., et al. (2008). A global map of human impact on marine ecosystems. *Science* 319, 948–952. doi: 10.1126/science.1149345
- Heery, E. C., Dafforn, K. A., Smith, J. A., Ushiyama, S., and Mayer-Pinto, M. (2018). Not all artificial structures are created equal: Pillings linked to greater ecological and environmental change in sediment communities than seawalls. *Mar. Environ. Res.* 142, 286–294. doi: 10.1016/j.marenvres.2018.08.012
- Heymans, J. J., Coll, M., Link, J. S., Mackinson, S., Steenbeek, J., Walters, C., et al. (2016). Best practice in Ecosim with Ecosim food-web models for ecosystem-based management. *Ecol. Model.* 331, 173–184. doi: 10.1016/j.ecolmodel.2015.12.007
- Hong, X., Chen, Z., Zhang, J., Jiang, Y., Gong, Y., Cai, Y., et al. (2022). Analysis of ecological carrying capacity of reef organisms in Qilianyu Islands based on Ecosim model. *J. Trop. Oceanography* 41, 15–27. doi: 10.11978/2020156
- Huang, M., Xu, S., Liu, Y., Xiao, Y., Wang, T., and Li, C. (2019). Assessment of ecological carrying capacity of Sparus macrocephalus in Daya Bay based on an ecosim model. *J. Fishery Sci. China* 26. doi: 10.3724/SP.J.1118.2019.18328
- Hughes, B. B., Beheshti, K. M., Tinker, M. T., Angelini, C., Endris, C., Murai, L., et al. (2024). Top-predator recovery abates geomorphic decline of a coastal ecosystem. *Nature* 626, 111–118. doi: 10.1038/s41586-023-06959-9
- Hughes, T., Bellwood, D., Folke, C., Steeneck, R., and Wilson, J. (2005). New paradigms for supporting the resilience of marine ecosystems. *Trends Ecol. Evol.* 20, 380–386. doi: 10.1016/j.tree.2005.03.022
- Jackson, J. B., Kirby, M. X., Berger, W. H., Bjorndal, K. A., Botsford, L. W., Bourque, B. J., et al. (2001). Historical overfishing and the recent collapse of coastal ecosystems. *Science* 293, 629–637. doi: 10.1126/science.1059199
- Jiang, W., and Gibbs, M. T. (2005). Predicting the carrying capacity of bivalve shellfish culture using a steady, linear food web model. *Aquaculture* 244, 171–185. doi: 10.1016/j.aquaculture.2004.11.050
- Jordán, F. (2009). Keystone species and food webs. *Philos. Trans. R. Soc. B: Biol. Sci.* 364, 1733–1741. doi: 10.1098/rstb.2008.0335
- Keramidas, I., Dimarchopoulou, D., Ofir, E., Scotti, M., Tsikliras, A. C., and Gal, G. (2023). Ectopath perspective in fisheries management: a review of Ecosim models in European marine ecosystems. *Front. Mar. Sci.* 10. doi: 10.3389/fmars.2023.1182921
- Krumhansl, K. A., and Scheibling, R. E. (2012). Production and fate of kelp detritus. *Mar. Ecol. Prog. Ser.* 467, 281–302. doi: 10.3354/meps09940
- Levin, L. A., Ekau, W., Gooday, A. J., Jorissen, F., Middelburg, J. J., Naqvi, S. W. A., et al. (2009). Effects of natural and human-induced hypoxia on coastal benthos. *Biogeosciences* 6, 2063–2098. doi: 10.5194/bg-6-2063-2009
- Libralato, S., Christensen, V., and Pauly, D. (2006). A method for identifying keystone species in food web models. *Ecol. Model.* 195, 153–171. doi: 10.1016/j.ecolmodel.2005.11.029
- Libralato, S., Coll, M., Tudela, S., Palomera, I., and Pranovi, F. (2008). Novel index for quantification of ecosystem effects of fishing as removal of secondary production. *Mar. Ecol. Prog. Ser.* 355, 107–129. doi: 10.3354/meps07224
- Lindeman, R. L. (1942). The trophic-dynamic aspect of ecology. *Ecology* 23, 399–417. doi: 10.2307/1930126
- Link, J. S. (2010). Adding rigor to ecological network models by evaluating a set of pre-balance diagnostics: A plea for PREBAL. *Ecol. Model.* 221, 1580–1591. doi: 10.1016/j.ecolmodel.2010.03.012
- Liu, H. (2022). *Study on influencing factors and countermeasures of marine ranching development in yantai* (Yantai University: Master).
- Liu, H., Huang, L., Tan, Y., Ke, Z., Liu, J., Zhao, C., et al. (2017). Seasonal variations of chlorophyll a and primary production and their influencing factors in the Pearl River Estuary. *J. Trop. Oceanography* 36, 81–91. Available online at: <https://www.jto.ac.cn/EN/10.11978/2016033>.
- Liu, H., Yang, C., Zhang, P., Li, W., and Zhang, X. (2019a). An Ecosim evaluation of system structure and function for the Laoshan Bay artificial reef zone ecosystem. *Acta Ecologica Sin.* 39, 3926–3936. Available online at: <https://www.ecologica.cn/html/2019/11/stxb201805301193.htm>.
- Liu, Y., Wu, Z., Yang, C., Shan, B., Liu, S., and Sun, D. (2019b). Ecological carrying capacity of six species of stock enhancement in Pearl River estuary based on Ecosim model. *South China Fisheries Sci.* 15, 19–28. doi: 10.12131/20180265
- Lobry, J., David, V., Pasquaud, S., Lepage, M., Sautour, B., and Rochard, E. (2008). Diversity and stability of an estuarine trophic network. *Mar. Ecol. Prog. Ser.* 358, 13–25. doi: 10.3354/meps07294
- Lomartire, S., Marques, J. C., and Gonçalves, A. M. M. (2021). The key role of zooplankton in ecosystem services: A perspective of interaction between zooplankton and fish recruitment. *Ecol. Indic.* 129. doi: 10.1016/j.ecolind.2021.107867
- Lynam, C. P., Llope, M., Möllmann, C., Helaoui, P., Bayliss-Brown, G. A., and Stenseth, N. C. (2017). Interaction between top-down and bottom-up control in marine food webs. *Proc. Natl. Acad. Sci.* 114, 1952–1957. doi: 10.1073/pnas.1621037114
- Mor, J. R., Muñoz, I., Sabater, S., Zamora, L., and Ruhi, A. (2021). Energy limitation or sensitive predators? Trophic and non-trophic impacts of wastewater pollution on stream food webs. *Ecology* 103. doi: 10.1002/ecy.3587
- Morissette, L., Hammill, M., and Savenkoff, C. (2006). The trophic role of marine mammals in the northern Gulf of St. Lawrence. *Mar. Mammal Sci.* 22, 74–103. doi: 10.1111/j.1748-7692.2006.00007.x
- Myers, R. A., Baum, J. K., Shepherd, T. D., Powers, S. P., and Peterson, C. H. (2007). Cascading effects of the loss of apex predatory sharks from a coastal ocean. *Science* 315, 1846–1850. doi: 10.1126/science.1138657
- Nauta, J., Christianen, M. J. A., Temmink, R. J. M., Fivash, G. S., Marin-Diaz, B., Reijers, V. C., et al. (2023). Biodegradable artificial reefs enhance food web complexity and biodiversity in an intertidal soft-sediment ecosystem. *J. Appl. Ecol.* 60, 541–552. doi: 10.1111/1365-2664.14348
- Odum, E. P. (1969). The Strategy of Ecosystem Development: An understanding of ecological succession provides a basis for resolving man's conflict with nature. *Science* 164, 262–270. doi: 10.1126/science.164.3877.262
- Palomares, M. L. D., and Pauly, D. (1998). Predicting food consumption of fish populations as functions of mortality, food type, morphometrics, temperature and salinity. *Mar. Freshw. Res.* 49, 447–453. doi: 10.1071/MF98015
- Pauly, D., and Christensen, V. (1995). Primary production required to sustain global fisheries. *Nature* 374, 255–257. doi: 10.1038/374255a0
- Pauly, D., Christensen, V., Dalsgaard, J., Froese, R., and Torres, F. (1998). Fishing down marine food webs. *Science* 279, 860–863. doi: 10.1126/science.279.5352.860
- Pauly, D., Christensen, V., and Walters, C. J. (2000). Ecosim, Ecospace and Ecospace as tools for evaluating ecosystem impact of fisheries. *Ices J. Mar. Sci.* 57, 697–706. doi: 10.1006/jmsc.2000.0726
- Pauly, D., and Palomares, M. L. D. (2005). Fishing down marine food web: it is far more pervasive than we thought. *Bull. Mar. Sci.* 76, 197–211.
- Pauly, D., Palomares, M., and Christensen, P. I. V. (1993). Improved construction, parametrization and interpretation of steady-state ecosystem models. *ICLARM Conf. Proc.* 26, 1–13.
- Peng, S., Lai, Z., and Mai, Y. (2019). Distribution of quantity and diversity of macrobenthos in the Pearl River Estuary. *Mar. Fisheries* 41, 266–277. doi: 10.13233/j.cnki.mar.fish.2019.03.002

- Pianka, E. R. (1973). The structure of lizard communities. *Annu. Rev. Ecology Evolution Systematics* 4, 53–74. doi: 10.1146/annurev.es.04.110173.000413
- Pikitch, E. K., Santora, C., Babcock, E. A., Bakun, A., Bonfil, R., Conover, D. O., et al. (2004). Ecosystem-Based Fishery Management. *Science* 305, 346–347. doi: 10.1126/science.1098222
- Pitt, K. A., Welsh, D. T., and Condon, R. H. (2009). Influence of jellyfish blooms on carbon, nitrogen and phosphorus cycling and plankton production. *Hydrobiologia* 616, 133–149. doi: 10.1007/s10750-008-9584-9
- Power, M. E., Tilman, D., Estes, J. A., Menge, B. A., Bond, W. J., Mills, L. S., et al. (1996). Challenges in the quest for keystones: identifying keystone species is difficult—but essential to understanding how loss of species will affect ecosystems. *BioScience* 46, 609–620. doi: 10.2307/1312990
- Purcell, J. E. (2003). Predation on zooplankton by large jellyfish, *Aurelia labiata*, *Cyanea capillata* and *Aequorea aequorea*, in Prince William Sound, Alaska. *Mar. Ecol. Prog. Ser.* 246, 137–152. doi: 10.3354/meps246137
- Rahman, M. F., Qun, L., Xiujuan, S., Chen, Y., Ding, X., and Liu, Q. (2019). Temporal changes of structure and functioning of the Bohai Sea Ecosystem: Insights from Ecopath Models. *Thalassas: Int. J. Mar. Sci.* 35, 625–641. doi: 10.1007/s41208-019-00139-1
- Reeds, K. A., Smith, J. A., Suthers, I. M., and Johnston, E. L. (2018). An ecological halo surrounding a large offshore artificial reef: Sediments, infauna, and fish foraging. *Mar. Environ. Res.* 141, 30–38. doi: 10.1016/j.marenvres.2018.07.011
- Ruzicka, J., Chiaverano, L., Coll, M., Garrido, S., Tam, J., Murase, H., et al. (2024). The role of small pelagic fish in diverse ecosystems: knowledge gleaned from food-web models. *Mar. Ecol. Prog. Ser.* 741, 7–27. doi: 10.3354/meps14513
- Salomon, A. K., Waller, N. P., McIlhagga, C., Yung, R. L., and Walters, C. (2002). Modeling the trophic effects of marine protected area zoning policies: A case study. *Aquat. Ecol.* 36, 85–95. doi: 10.1023/A:1013346622536
- Saygu, İ., Thurstan, R. H., Roberts, C., Heard, Z., Akoglu, E., and Halloran, P. R. (2025). Historical ecosystem models can serve as a baseline for indicator-based assessment: the North Sea. *Front. Mar. Sci.* 12. doi: 10.3389/fmars.2025.1646031
- Searles, A. R., Gipson, E. E., Walters, L. J., and Cook, G. S. (2022). Oyster reef restoration facilitates the recovery of macroinvertebrate abundance, diversity, and composition in estuarine communities. *Sci. Rep.* 12. doi: 10.1038/s41598-022-11688-6
- Shannon, C. E. (1948). A mathematical theory of communication. *Bell System Tech. J.* 27, 379–423. doi: 10.1002/j.1538-7305.1948.tb01338.x
- Shi, J., Wang, T., Li, C., Zhao, J., Kang, Z., Song, X., et al. (2024). Food web structure and trophic diversity for the fishes of four islands in the Pearl River Estuary, China. *Ecol. Indic.* 160, 111916. doi: 10.1016/j.ecolind.2024.111916
- Si, Y. (2018). *Study on mesozooplankton grazing and reproduction in Pearl River estuary and north-central South China Sea* (Xiamen University: Master).
- Sobczak, W. V., Cloern, J. E., Jassby, A. D., Cole, B. E., Schraga, T. S., and Arnsberg, A. (2005). Detritus fuels ecosystem metabolism but not metazoan food webs in San Francisco estuary's freshwater delta. *Estuaries* 28, 124–137. doi: 10.1007/BF02732759
- Song, M., Wang, J., Nie, Z., Wang, L., Wang, J., Zhang, J., et al. (2022). Evaluation of artificial reef habitats as reconstruction or enhancement tools of benthic fish communities in northern Yellow Sea. *Mar. Pollut. Bull.* 182. doi: 10.1016/j.marpolbul.2022.113968
- Sun, L., Lin, Y., Chen, L., Cao, W., and Zheng, L. (2016). Analysis of ecosystem structure and function in the northern Beibu Gulf VII: Nutrition structure and keystone species selection based on Ecopath with Ecosim. *J. Trop. Oceanography* 35, 51–62. doi: 10.11978/2015113
- Susini, L., and Todd, V. L. G. (2021). Predictive capacity of Ecopath with Ecosim: Model performance and ecological indicators' response to imprecision. *Environ. Model. Software* 143. doi: 10.1016/j.envsoft.2021.105098
- Tanaya, T., Iwamura, S., Okada, W., and Kuwae, T. (2025). Artificial structures can facilitate rapid coral recovery under climate change. *Sci. Rep.* 15. doi: 10.1038/s41598-025-93531-2
- Tang, Q. (1996). On the carrying capacity and its study. *Prog. Fishery Sci.* 17, 1–6.
- Ulanowicz, R., and Puccia, C. (1990). Mixed trophic impacts in ecosystems. *Coenoses* 7–16.
- Valentine, J. F., Heymans, J. J., Coll, M., Libralato, S., Morissette, L., and Christensen, V. (2014). Global patterns in ecological indicators of marine food webs: A modelling approach. *PLoS One* 9. doi: 10.1371/journal.pone.0095845
- Walters, C. J., Martell, S. J. D., Christensen, V., and Mahmoudi, B. (2008). An ecosim model for exploring gulf of Mexico ecosystem management options: implications of including multistanza life-history models for policy predictions. *Bull. Mar. Sci.* 83, 251–271.
- Wang, X., Feng, J., Lin, C., Liu, H., Chen, M., and Zhang, Y. (2022a). Structural and functional improvements of coastal ecosystem based on artificial oyster reef construction in the bohai sea, China. *Front. Mar. Sci.* 9. doi: 10.3389/fmars.2022.829557
- Wang, Z., Feng, J., Lozano-Montes, H. M., Loneragan, N. R., Zhang, X., Tian, T., et al. (2022b). Estimating ecological carrying capacity for stock enhancement in marine ranching ecosystems of Northern China. *Front. Mar. Sci.* 9. doi: 10.3389/fmars.2022.936028
- Wang, Y., Hu, J., Pan, H., Li, S., and Failler, P. (2016). An integrated model for marine fishery management in the Pearl River Estuary: Linking socio-economic systems and ecosystems. *Mar. Policy* 64, 135–147. doi: 10.1016/j.marpol.2015.11.014
- Wang, X., Lin, C., Wang, W., and Zhang, L. (2024b). The non-negligible contribution of foundation species to artificial reef construction revealed by Ecopath models. *J. Environ. Manage.* 366. doi: 10.1016/j.jenvman.2024.121887
- Wang, Z., Yao, L., Yu, J., Chen, P., Li, Z., and Yang, W. (2024c). Evaluation of the ecological carrying capacity of Wailingding marine ranching in Zhuhai, China by high-resolution remote sensing. *Front. Mar. Sci.* 11. doi: 10.3389/fmars.2024.1354407
- Wang, P., Zhang, F., Guo, D., Chi, X., Feng, S., and Sun, S. (2024a). Trophic effects of jellyfish blooms on fish populations in ecosystems of the coastal waters of China. *Sci. Total Environ.* 948, 174832. doi: 10.1016/j.scitotenv.2024.174832
- Ware, D. M., and Thomson, R. E. (2005). Bottom-up ecosystem trophic dynamics determine fish production in the northeast pacific. *Science* 308, 1280–1284. doi: 10.1126/science.1109049
- Wenhui, C., Bingqing, X., Xiuqiang, D., Jisong, Y., Min, L., Depu, Z., et al. (2025). Comparative study of the characteristics of the energy flow and food web structure in the Laizhou Bay ecosystem based on the Ecopath and LIM-MCMC models. *Front. Mar. Sci.* 12. doi: 10.3389/fmars.2025.1572355
- Xie, X., Chen, P., Tong, F., Yuan, H., Feng, X., Yu, J., et al. (2022). Site selection of marine ranching in Wailingding Island sea area of Zhuhai. *South China Fisheries Sci.* 18, 18–29. doi: 10.12131/20210241
- Yan, J., Chen, Y., Cao, Y., Sun, J., Wen, B., Gao, X., et al. (2025). Marine ranching enhances ecosystem stability and biological carbon sequestration potential: insights from Ecopath with Ecosim model simulation of 30-year ecological path of a national marine ranching in China. *Front. Mar. Sci.* 12. doi: 10.3389/fmars.2025.1583896
- Yao, Y., and Chen, N. (2021). Biodiversity of phytoplankton and red tide species in the Pearl River Estuary. *Mar. Sci.* 45, 75–90. Available online at: http://qdhy.ijournal.cn/hyksen/ch/reader/view_abstract.aspx?file_no=20210909&flag=1.
- Yuan, J., and He, Y. (2022). Construction and positive research of comprehensive development evaluation index system of marine ranching. *Ocean Dev. Manage.* 39, 93. doi: 10.20016/j.cnki.hykyfjgl.2022.12.001
- Yuan, D., Qiu, M., Zhou, X., Zhang, Y., and Zhao, J. (2024). Study on the structure and energy flow of the salt marsh wetland ecosystem in Liaohai Estuary based on the Ecopath model. *Front. Mar. Sci.* 11. doi: 10.3389/fmars.2024.1487370
- Yuan, M., Tang, Y., Xu, S., Chen, Z., Yang, Y., and Jiang, Y. (2017). Community structure of fishery resources from the Nansha waters of Pearl River Estuary in autumn. *South China Fisheries Sci.* 13, 18–25. doi: 10.3969/j.issn.2095-0780.2017.02.003
- Zeng, Z., Cheung, W. W. L., Lai, H., Yi, H., Bi, S., Li, H., et al. (2022). Species and functional dynamics of the demersal fish community and responses to disturbances in the pearl river estuary. *Front. Mar. Sci.* 9. doi: 10.3389/fmars.2022.921595
- Zhang, J., Gao, Y., and Fang, H. (2011). Abundance and biomass of meiobenthos in Lingdingyang Bay of Pearl River Estuary. *Chin. J. Appl. Ecol.* 22, 2741–2748. doi: 10.13287/j.1001-9332.2011.0392
- Zhang, P., Zhang, H., Wang, S., Woodward, G., O'Gorman, E. J., Jackson, M. C., et al. (2025). Multiple stressors simplify freshwater food webs. *Global Change Biol.* 31. doi: 10.1111/gcb.70114
- Zhang, R., Zhang, Q., Zhao, J., Wu, Z., Liu, H., Shou, L., et al. (2022). Using ecopath models to explore differences in ecosystem characteristics between an artificial reef and a nearby natural reef on the coast of the north yellow sea, China. *Front. Mar. Sci.* 9. doi: 10.3389/fmars.2022.911714
- Zhou, W., Ding, D., Suo, A., He, W., and Tian, T. (2021). Key functional groups in marine ranching fishery resources from the Pearl River Estuary. *J. Fisheries China* 45, 433–443. doi: 10.11964/jfc.20191212111